

Comparing Pythia Output with Data

A Preliminary Look - Version II

Alex R. Dzierba

Introduction

This is a preliminary look at Monte Carlo data simulated by Pythia comparing it to published data¹. I am using Pythia parameters as tuned by Eugene Chudakov and Elke Aschenauer and as passed on to me by David Lawrence. I generated 10^5 events with $E_\gamma = 9$ GeV. This is a work in progress and this note will be updated.

Distribution in particle types

The distribution in final state particle types, using the GEANT-based numbering scheme is shown in Figure 1. Note that the vertical scale is logarithmic. This distribution is repeated in Figure 2(a) but now with a linear scale along the distribution in numbers of particles, numbers of charged particles and numbers of photons (in Figure 2(b) through (d) respectively).

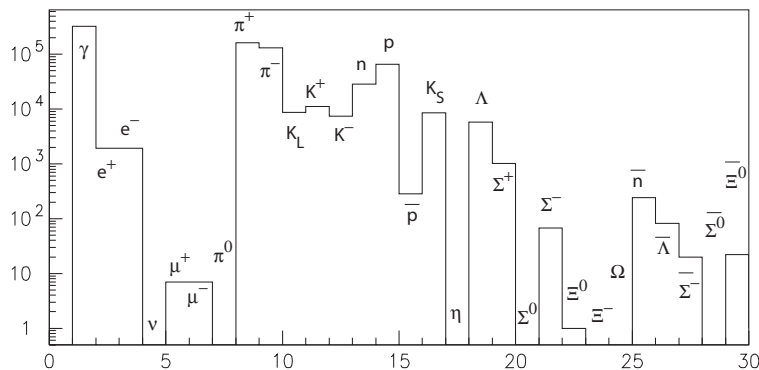


Figure 1: Distribution of types of final state particles from the Pythia simulation.

Distribution among topologies

Ratios of cross sections for various topologies for an incident photon energy of 9 GeV are summarized in Table 1. The agreement is quite good.

Three-prong sample

No neutrals: Distributions for Pythia data corresponding to $\gamma p \rightarrow \pi^+ \pi^- p$ are shown in Figure 3. At 9 GeV $\gamma p \rightarrow \rho^0 p$ accounts for 92% of $\gamma p \rightarrow \pi^+ \pi^- p$ for data, consistent with Pythia simulations. The

¹Cross sections at GlueX energies are summarized in A. Dzierba, GlueX-doc-825.

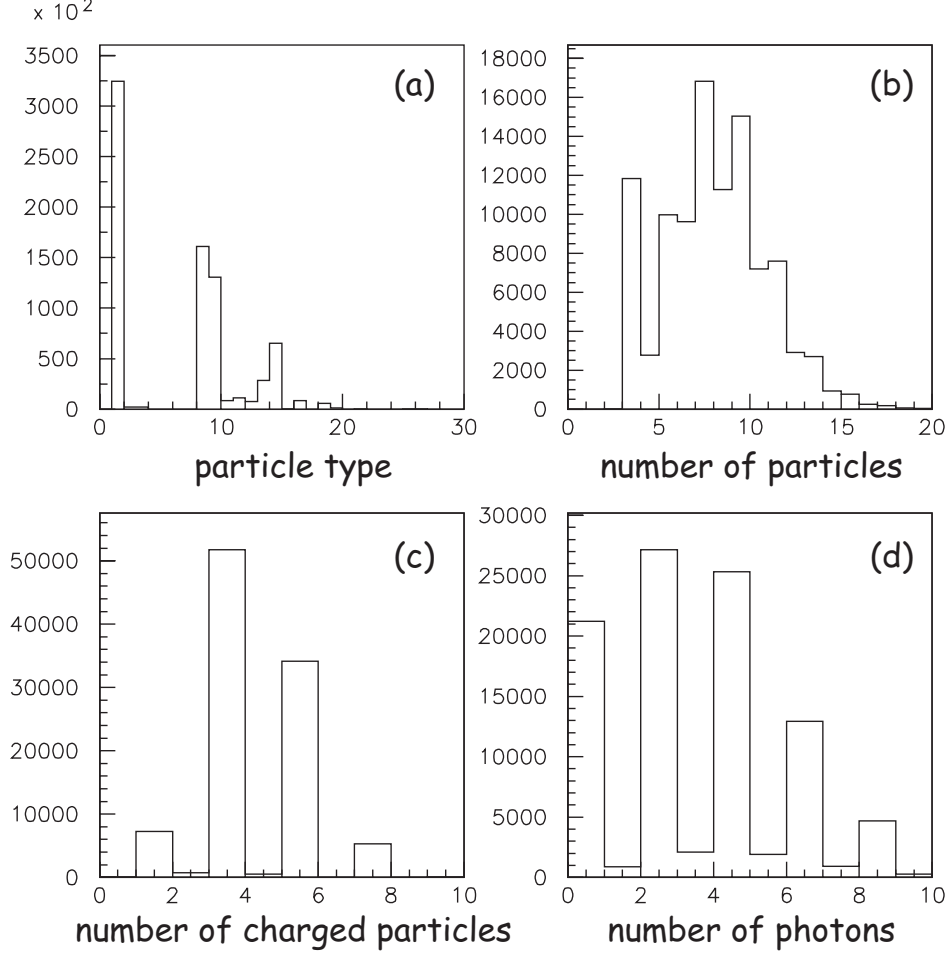


Figure 2: (a) Same as Figure 1 but with a linear vertical scale; (b) Distribution in the number of particles; (c) Distributions of number of charged particles; and (d) Distribution in the number of photons.

2π effective mass distribution is shown in Figure 3(a) and the π^+p and π^-p effective mass distributions are shown in Figures 3(b) and (c). For the $|t|$ distribution (Figure 3(d)), a fit to $dN/d|t| \propto e^{-a|t|}$ yields $a = 7.4 \pm 0.8 \text{ GeV}^{-2}$ for the Pythia data compared to published data for which $a = 6.5 \pm 0.5 \text{ GeV}^{-2}$.

Single π^0 : Distributions for Pythia data corresponding to $\gamma p \rightarrow \pi^+\pi^-\pi^0p$ are shown in Figure 4. Figure 4(a) shows the $\pi^+\pi^-\pi^0$ effective mass distribution with the ω clearly seen. Figure 4(b) shows the 2π effective mass distribution for three possible combinations – the ρ is clearly seen and the lower peak is due to the ω decays. Figure 4(c) shows the πp effective mass distribution for three possible combinations – the Δ is clearly seen. Published data at 9 GeV yield cross sections for ωp , $\rho^-\Delta^{++}$, $\rho^0\Delta^+$ and $\rho^+\Delta^0$ of $1.9 \pm 0.3 \mu\text{b}$, $1.1 \pm 0.2 \mu\text{b}$, $0.3 \pm 0.2 \mu\text{b}$ and $0.2 \pm 0.2 \mu\text{b}$ respectively. Pythia clearly accounts for baryon resonance production. Figure 4(d) Distribution in momentum transfer squared from the incident photon to the 3π system.

Multi-neutrals: Distributions for Pythia data corresponding to $\gamma p \rightarrow 3$ prongs at 9 GeV are shown in Figure 5. Figures 5(a) and (b) show the distribution in particle type and the number of photons respectively. Figures 5(c) and (d) show the missing mass recoiling against the three charged particles. Figures 5(d) missing mass distribution for the lower masses and with a logarithmic scale. The peak at zero mass are

Table 1: Ratios of cross sections for various topologies for an incident photon energy of 9 GeV.

Ratio	Pythia (%)	Data (%)
$\sigma(1\text{-prong})/\sigma_{total}$	7.1	6.9 ± 0.9
$\sigma(3\text{-prong})/\sigma_{total}$	51.8	51.7 ± 1.2
$\sigma(5\text{-prong})/\sigma_{total}$	34.1	27.6 ± 0.7
$\sigma(7\text{-prong})/\sigma_{total}$	5.4	5.5 ± 0.2
$\sigma(9\text{-prong})/\sigma_{total}$	0.3	0.5 ± 0.06
$\sigma(\pi^+\pi^-p)/\sigma(3\text{-prong})$	21	23 ± 1
$\sigma(\pi^+\pi^-\pi^0p)/\sigma(3\text{-prong})$	9	11 ± 1
$\sigma(\omega p)/\sigma(\pi^+\pi^-\pi^0p)$	24	25 ± 4

$\pi^-\pi^+p$ events. Peaks corresponding to recoil π^0 , K_S , η and neutron are also seen.

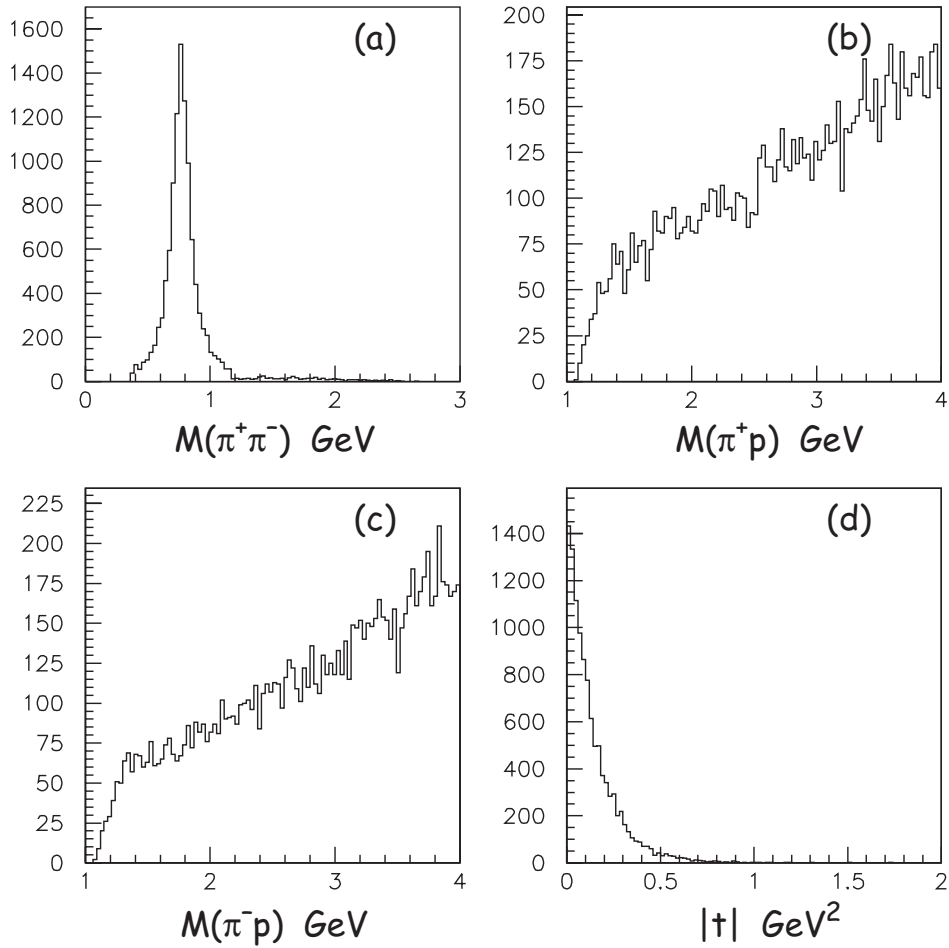


Figure 3: Distributions for Pythia data corresponding to $\gamma p \rightarrow \pi^+\pi^-p$ at 9 GeV. (a) The $\pi^+\pi^-$ effective mass distribution showing the ρ^0 ; (b) and (c) The π^+p and π^-p effective mass distributions; (d) Distribution in momentum transfer squared from the incident photon to the 2π system.

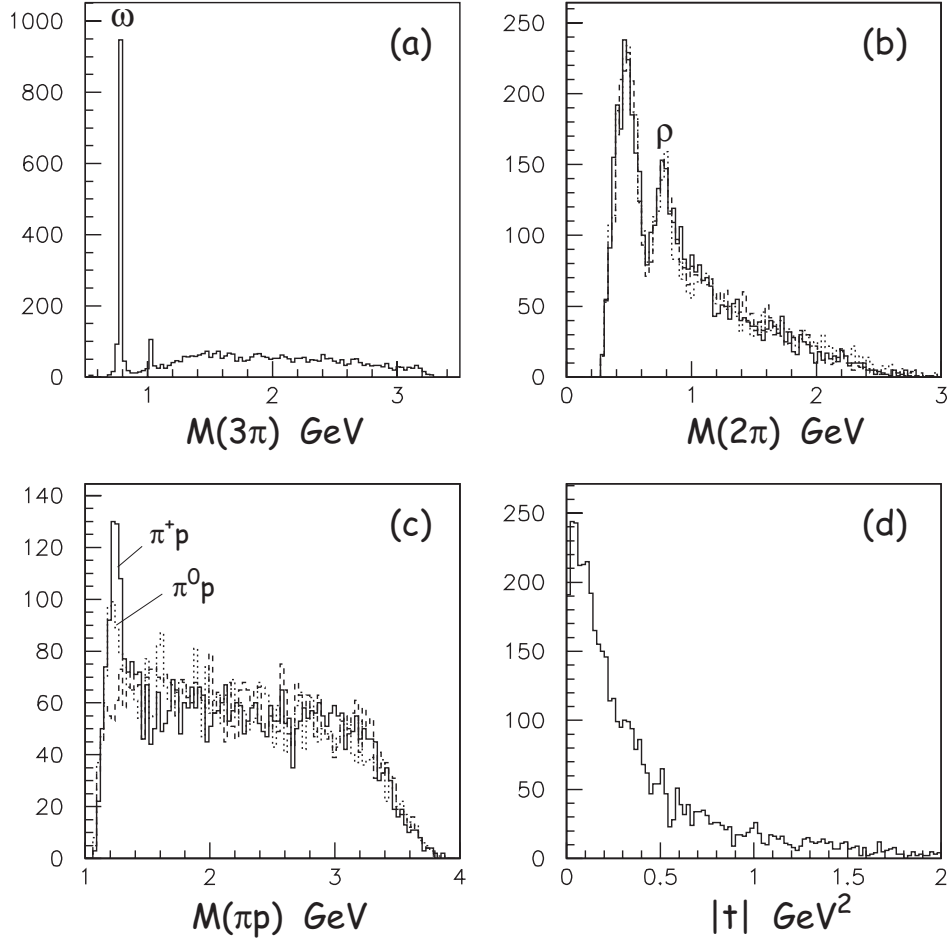


Figure 4: Distributions for Pythia data corresponding to $\gamma p \rightarrow \pi^+ \pi^- \pi^0 p$ at 9 GeV. (a) The $\pi^+ \pi^- \pi^0$ effective mass distribution showing the ω ; (b) The 2π effective mass distribution for three possible combinations – the ρ is clearly seen; (c) The πp effective mass distribution for three possible combinations – the Δ is clearly seen; (d) Distribution in momentum transfer squared from the incident photon to the 3π system.

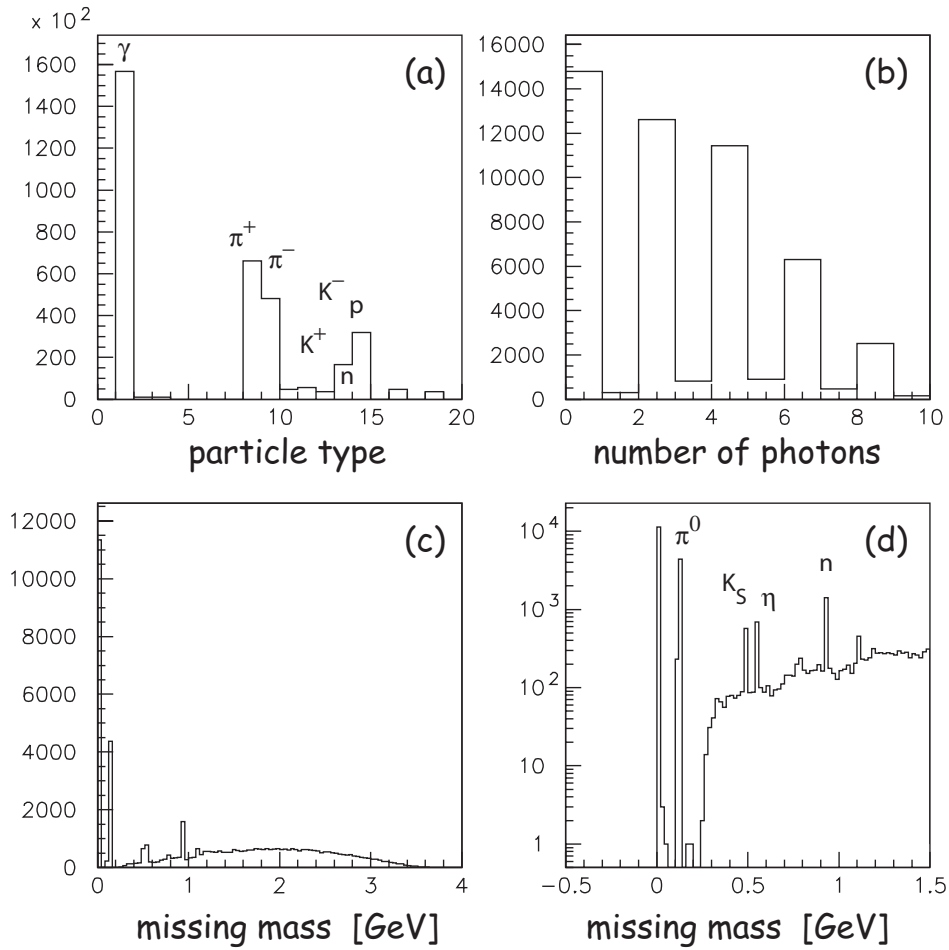


Figure 5: Distributions for Pythia data corresponding to $\gamma p \rightarrow 3$ prongs at 9 GeV. (a) Distribution in particle type; (b) Distribution in number of photons; (c) Missing mass recoiling against the three charged particles; (d) Missing mass distribution shown for the lower masses and with a logarithmic scale. The peak at zero mass are $\pi^- \pi^+ p$ events. Peaks corresponding to recoil π^0 , K_S , η and neutron are also seen.